HHS Public Access

Author manuscript

Osteoarthritis Cartilage. Author manuscript; available in PMC 2021 November 01.

Published in final edited form as:

Osteoarthritis Cartilage. 2020 November ; 28(11): 1459–1470. doi:10.1016/j.joca.2020.08.003.

Heparan sulfate deficiency leads to hypertrophic chondrocytes by increasing bone morphogenetic protein signaling

K. Kawashima[†], **H. Ogawa**[†], **S. Komura**[†], **T. Ishihara**[‡], **Y. Yamaguchi**[§], **H. Akiyama**[†], **K. Matsumoto**[†,*]

[†]Department of Orthopaedic Surgery, Gifu University Graduate School of Medicine, 1-1 Yanagido, Gifu, Japan

[‡]Innovative and Clinical Research Promotion Center, Gifu University Hospital, 1-1 Yanagido, Gifu, Japan

[§]Human Genetics Program, Sanford Burnham Prebys Medical Discovery Institute, 10901 North Torrey Pines Road, La Jolla, CA, 92037, USA

SUMMARY

Objective: Exostosin-1 (*EXT1*) and *EXT2* are the major genetic etiologies of multiple hereditary exostoses and are essential for heparan sulfate (HS) biosynthesis. Previous studies investigating HS in several mouse models of multiple hereditary exostoses have reported that aberrant bone morphogenetic protein (BMP) signaling promotes osteochondroma formation in *Ext1*-deficient mice. This study examined the mechanism underlying the effects of HS deficiency on BMP/Smad signaling in articular cartilage in a cartilage-specific $Ext^{-/-}$ mouse model.

Method: We generated mice with a conditional *Ext1* knockout in cartilage tissue (*Ext1*-cKO mice) using *Prg4-Cre* transgenic mice. Structural cartilage alterations were histologically evaluated and phospho-Smad1/5/9 (pSmad1/5/9) expression in mouse chondrocytes was analyzed. The effect of pharmacological intervention of BMP signaling using a specific inhibitor was assessed in the articular cartilage of *Ext1*-cKO mice.

[*]Address correspondence and reprint requests to: K. Matsumoto, Department of Orthopedic Surgery, Gifu University Graduate School of Medicine, 1-1 Yanagido, Gifu, 501-1194, Japan. Tel.: 81-58-230-6333; Fax: 81-58-230-6334. mkazuu@gifu-u.ac.jp (K. Matsumoto).

Contributions

KK acquired the data, performed most of the data analysis, and drafted the manuscript. KM, HO, SK, TI, YY, and HA helped interpret the data and assisted in the preparation of the manuscript. TI assisted with the statistical analysis. KM was involved in the conception and design of the study, the analysis and interpretation of the data, and in drafting the manuscript. All other authors contributed to the data collection and interpretation and critically reviewed the manuscript. All authors approved the final version of the manuscript.

Conflict of interest

Kenji Kawashima: no conflicts of interest to declare.
Hiroyasu Ogawa: no conflicts of interest to declare.
Shingo Komura: no conflicts of interest to declare.
Takuma Ishihara: no conflicts of interest to declare.
Yu Yamaguchi: no conflicts of interest to declare.
Haruhiko Akiyama: no conflicts of interest to declare.
Kazu Matsumoto: no conflicts of interest to declare.

Supplementary data

Supplementary data to this article can be found online at https://doi.org/10.1016/j.joca.2020.08.003.

Results: Hypertrophic chondrocytes were significantly more abundant ($P = 0.021$) and cartilage thickness was greater in *Ext1*-cKO mice at 3 months postnatal than in control littermates ($P = 0.036$ for femur; and $P < 0.001$ for tibia). However, osteoarthritis did not spontaneously occur before the 1-year follow-up. MMP-13 and ADAMTS-5 were upregulated in hypertrophic chondrocytes of transgenic mice. Immunostaining and western blotting revealed that pSmad1/5/9-positive chondrocytes were more abundant in the articular cartilage of *Ext1*-cKO mice than in control littermates. Furthermore, the BMP inhibitor significantly decreased the number of hypertrophic chondrocytes in *Ext1*-cKO mice ($P = 0.007$).

Conclusions: HS deficiency in articular chondrocytes causes chondrocyte hypertrophy, wherein upregulated BMP/Smad signaling partially contributes to this phenotype. HS might play an important role in maintaining the cartilaginous matrix by regulating BMP signaling.

Keywords

Heparan sulfate; Chondrocyte; Hypertrophy; Bone morphogenetic protein signaling; Ext1; Prg4

Introduction

Multiple hereditary exostoses (MHE) is a relatively rare autosomal-dominant skeletal disorder characterized by the formation of multiple cartilage-capped bony protrusions (osteochondroma) and characteristic bone deformities. The exostosin-1 (*EXT1*) and exostosin-2 (*EXT2*) genes, which encode heparan sulfate (HS) glycosyltransferases, are major genetic etiologies of MHE. *EXT1* is located on chromosome 8q23–q24, whereas *EXT2* is on chromosome 11p11–p12, and these genes are essential for HS chain elongation. The HS chain backbone can be synthesized by the co-operative actions of both *EXT1* and *EXT2*, each of which cannot compensate for deficiency of the other[1]. Several reports have described mutational variations and novel mutations in *EXT1* and *EXT2* in patients with MHE from several different countries[2–6]. Patients with MHE exhibit various skeletal deformities including short stature, limb-length inequalities, bowing of the limb bones, scoliosis, and early-onset osteoarthritis (OA)[7–9]. A recent study reported that HS loss is an important determinant of the ratio of peripheral and longitudinal growth, and osteochondromas interfering with growth plate function likely cause several skeletal deformities[10]. Furthermore, mice with a knockout of exon 3 of perlecan, a large HS proteoglycan present in cartilage, displayed a chondroprotective phenotype in the articular cartilage[11]. We previously reported that stochastic *Ext1* inactivation in a small fraction of *Col2a1*-expressing cells, using a *Col2a1-CreERT* transgene and the loxP-modified allele *Ext1*^{flox12} (*Col2a1-CreERT;Ext1*$^{f/f}$ mice), resulted in multiple osteochondromas and skeletal deformities in mice that closely resemble the human MHE phenotype[13]. These mice displayed mild abnormalities in the growth plate and hypertrophy-like changes in the articular cartilage. Accordingly, we hypothesized that chondrocyte hypertrophy in the articular cartilage is accelerated by HS deficiency and that HS plays an important role in maintaining the cartilaginous matrix.

Chondrocyte hypertrophy is a commonly observed characteristic of OA in humans[14–17]. Hypertrophic chondrocyte differentiation is characterized by the upregulation of type X collagen[18] and matrix metalloproteinase (MMP-13)[19]. These changes play a crucial role in

OA progression by driving protease-mediated cartilage degradation[20]. Chondrocyte hypertrophy is not stringently regulated by a single pathway, but rather appears to be regulated by an intricate network composed of multiple signaling pathways, involving the wingless-type MMTV integration site (WNT) protein, bone morphogenetic proteins (BMPs)/transforming growth factor-β (TGFβ), parathyroid hormone-related peptide, Indian hedgehog (Ihh) protein, fibroblast growth factors (FGFs), insulin-like growth factor, and hypoxia-inducible factors[21].

Enhanced bone morphogenetic protein (BMP) signaling owing to HS suppression plays a role in osteochondroma formation in MHE[22–24]. Huegel *et al.*[25] reported broad, ectopic excess BMP signaling in the perichondrium of long-bone growth plates in conditional *Ext1*-null mice, followed by ectopic cartilage tissue formation and osteochondroma development. Inubushi *et al.*[23] reported that aberrant perichondrial BMP signaling in progenitor cells in the perichondrium mediates osteochondromagenesis in a mouse model of MHE. Furthermore, pharmacological intervention of BMP signaling using a BMP-type I receptor inhibitor reduces osteochondroma formation in MHE mouse models[23,24]. Here, we focused on the biological role of HS through BMP/Smad signaling, particularly in articular chondrocytes. We analyzed the effects of HS deficiency on articular chondrocytes in mutant mice with the cartilage-specific deletion of *Ext1*.

Method

Mice

The experimental design and study protocols were approved by the animal experiment committees of Gifu University and were performed in compliance with the Animal Research: Reporting of *in Vivo* Experimental (ARRIVE) guidelines. The loxP-modified *Ext1* allele and the *Ext1*$^{f/f}$ mouse line were established as previously described[11]. Furthermore, a mouse line with the cartilage-specific deletion of *Ext1* was generated using *Prg4-Cre* transgenic mice [Fig. 1(A)]. From these two lines, conditional-knockout *Ext1*-mutant mice (*Prg4-Cre;Ext1*$^{f/f}$; referred to here as *Ext1*-cKO mice) were generated. Littermates that inherited an incomplete combination of the aforementioned alleles were used as controls (referred to here as wild-type (WT) mice). *Rosa26*-lacZ (*R26R*) mice[26] were obtained from The Jackson Laboratory (Bar Harbor, ME, USA). Furthermore, we generated triple compound *Ext1*$^{f/f}$*;Prg4-Cre* mice in an *R26R* background to monitor Cre-mediated expression patterns through X-gal staining. All experiments were conducted with mice in a complete C57BL/6 background. Genotyping for *Ext1* and the *Cre* transgene was performed via PCR, as previously described[12].

Establishment of a mouse model of OA through destabilization of the medial meniscus (DMM)

The surgically-induced OA model was generated in the right knee joint through destabilization of the medial meniscus (DMM) surgery, as described by Glasson *et al.*[27]. The contralateral left knee joint was sham-operated through the same approach without any ligament transection. The surgery was microscopically performed with general anesthesia. Four male *Ext1*-cKO mice and four male control littermates (control) finally underwent

DMM and sham surgery at the age of 10 weeks. At 8 weeks after DMM surgery, animals in the two groups were euthanized and subjected to histological evaluation.

Drug administration

For experiments involving the inhibitor of BMP signaling LDN-193189 (Sigma–Aldrich, St. Louis, MO, USA), the drug was synthesized as previously described[28]. *Ext1*-cKO mice were treated with an intra-peritoneal injection of 10 mg/kg LDN-193189, and vehicle-treated mutant littermates constituted the control group ($n = 4$ mice in both groups). The drug dose was similar to that successfully used in a previous study[23]. The initial injection was administered on postnatal day 14 (P14), and the second and subsequent injections were administered every other day for 3 weeks. Thereafter, the mice were euthanized and used for whole-mount skeletal preparation and histological analysis.

Analysis of the skeleton

For whole-mount analysis of the skeletons, mice were eviscerated and fixed in 95% ethanol overnight. The preparations were stained with 0.05% Alcian blue at pH 2.5 for 1–3 d, rinsed in 95% ethanol, incubated in 2% KOH for 1–24 h, and stained with 0.015% Alizarin red at pH 4.2 for 1–3 d. The stained preparations were cleaned in 20% glycerol/1% KOH for 5–14 d and transferred to 50% glycerol/50% ethanol for photography and storage. Radiographic examination was performed with a Faxitron cabinet X-ray system (Model 43855D, Faxitron X-Ray LLC, Lincolnshire, IL, USA), using an energy of 26 kV and exposure time of 10 s.

Histological assessment

Tissue specimens were dissected and fixed overnight in 4% paraformaldehyde (PFA), decalcified with EDTA for 10–14 d, and embedded in paraffin. Serial 6-μm-thick sections were processed for staining with Safranin O/Fast Green to examine cartilage. Articular cartilage pathology was evaluated using a scoring system designed to assess OA histology in mouse joints. To assess cartilage damage, sections were scored by two independent observers (K.K. and K.M.) using the Osteoarthritis Research Society International (OARSI)-recommended histologic grading system[29], and scores for the medial femoral condyle and medial tibial plateau were summed. Inter-observer repeatability was analyzed based on the intra-class correlation coefficient (ICC). Furthermore, the cartilage chondrocytes and hypertrophic chondrocytes were enumerated. The percentages of hypertrophic chondrocytes (%HC) in both the femoral condyle and tibial plateau were determined[30]. Cartilage thickness from the articular surface to the chondro-osseous junction of each section was defined as the average value of 10 manual thickness measurements obtained at regular intervals perpendicular to the cartilage surface[31]. Articular cartilage thickness was determined using ImageJ software (National Institutes of Health, Bethesda, MD, USA). In total, four mice were assessed in the control and *Ext1*-cKO groups at postnatal day 0 (P0), P14, postnatal month 1 (P1M), P3M, P6M, and P12M.

Immunohistochemistry

Sections were pretreated and subsequently treated at 4°C overnight with antibodies against type-II collagen (ab34712, Abcam, Cambridge, UK), type-X collagen (LSL-LB-0092,

Cosmo Bio, Tokyo, Japan), MMP-13 (18165-1-AP, Proteintech, Chicago, IL, USA), ADAMTS-5 (ab41037, Abcam), or phospho-Smad1/5/9 (#13820, Cell Signaling Technology, Danvers, MA, USA). After rinsing, the sections were incubated with a biotinylated anti-rabbit secondary antibody contained in the HRP/DAB Detection IHC Kit (Abcam) in accordance with the manufacturer's instructions for colorimetric visualization. Counterstaining was performed with hematoxylin. Negative controls were performed with normal rabbit IgG antibodies (I-1000, Vector lab, USA) under the same conditions.

X-gal staining

Whole-skeleton X-gal staining was performed as previously described[11]. Tissue specimens were rapidly dissected and pre-fixed in 4% PFA for 1 h at room temperature (15–25°C). Specimens were then incubated overnight at 4°C in the dark in 0.1% X-gal reaction buffer at pH 7.5, rinsed in PBS, post-fixed in 4% PFA overnight at 4°C, embedded in paraffin, decalcified in EDTA, and sectioned at a 6-μm thickness. Sections were counter-stained with nuclear fast red.

Terminal deoxynucleotidyl transferase dUTP nick end labeling (TUNEL) analysis

Transferase dUTP nick end labeling (TUNEL) staining was performed for knee joint sections of *Ext1*-cKO mice and control littermates ($n = 4$ per genotype) using a staining kit (Roche, Basel, Switzerland) in accordance with the manufacturer's instructions to detect apoptotic chondrocytes.

PCR experiments

Genomic DNA was extracted from various tissues using a Mighty Amp Genotyping Kit (Takara Bio, Shiga, Japan). For routine genotyping of animals, PCR was performed with an initial 2-min heating step at 98°C, followed by 30 cycles of denaturation for 10 s at 98°C, annealing for 15 s at 65°C, and extension for 1 min at 68°C. Primer #51 (5′-GGAGTGTGGATGAGTTGAAG-3′) and #52 (5′-CAACACTTTCAGCTCCAGTC-3′) were used to detect the $Ext1^{flox}$ allele.

Chondrocyte culture and western blotting

Murine articular chondrocytes were harvested from the knees and femoral head cartilage of and *Ext1*-cKO mice and control littermates ($n = 6$ per genotype) at P14 and cultured as previously described[32]. Total protein was extracted from chondrocyte samples using ice-cold RIPA lysis buffer containing protease and phosphatase inhibitors (Thermo Fisher Scientific, Waltham, MA, USA). Samples containing equal amounts of protein were resolved through SDS-PAGE (10% resolving gel) and electro-transferred onto nitrocellulose membranes (Bio-Rad, Laboratories, Hercules, CA, USA). The membranes were probed with antibodies against phospho-Smad1/5/9 (#13820; Cell Signaling Technology), Smad1 (#6944; Cell Signaling Technology), or GAPDH (#2188; Cell Signaling Technology). The immunoreactive proteins were visualized using ImmunoStar Zeta chemiluminescence reagent (FUJIFILM Wako Pure Chemical Corporation, Osaka, Japan). Signal intensities were quantified using ImageJ software and assessed relative to GAPDH expression as previously described[24,33].

Statistical analysis

The results are represented as the mean ± SD. Experiments were repeated independently at least three times, and representative data are shown. All comparisons between groups were conducted using the paired two-tailed *t*-test. We have selected this particular test since mice in *Ext1*-cKO and control groups were littermates, considered to be highly correlated, rather than independent. On the other hand, mice at different ages were considered independent since they were generated from different parents. Therefore, time-dependent changes were confirmed using a mixed-effects model with paired individuals as the random effect: time-dependent differences were confirmed via the global test for interaction, and differences in group means and between different ages were assessed via the test for main effect, respectively. A two-sided *P*-value less than 0.05 was considered to reflect statistically significant differences. All analyses were performed using the GraphPad Prism software version 8.0 (GraphPad, Inc., La Jolla, CA, USA) and R software version 3.6.2 (www.r-project.org).

Results

Cre-mediated recombination in superficial articular chondrocytes from Prg4-Cre mice

Previously, when examining the roles of HS in articular cartilage, we noted that lubricin (a secreted proteoglycan encoded by *PRG4*) was abundantly expressed by superficial articular chondrocytes[34]. Herein, we generated a mouse model with the cartilage-specific deletion of *Ext1* using *Prg4-Cre* transgenic mice. To verify the *Cre*-mediated expression patterns, we first analyzed *R26R* mice (hereafter called controls) and *R26R;Prg4-Cre* mice (hereafter identified cKO mice). One month after birth, we prepared serial longitudinal sections of the knees and processed them for histochemical staining with X-gal. In the knee joint, we observed *Cre*-mediated recombination in articular surface chondrocytes of *R26R;Prg4-Cre* mice [Fig. 1(B), (E)]. However, no evidence of recombination was obtained in the growth plate cartilage [Fig. 1(F)]. *Prg4* was expressed in other parts of the body, including the patellar tendons [Fig. 1(B)], costal cartilage (arrowheads, Fig. 1(C), (G)), and Achilles tendons [Fig. 1(D), (H)]. These findings are consistent with previous reports showing that Prg4/lubricin is expressed in articular cartilage and tendons, but not in growth plate cartilage[35,36]. Overall, these findings show that successful recombination occurred in *Prg4-Cre* transgenic mice.

Ext1-cKO mice exhibit hypertrophic chondrocytes in articular cartilage tissue and osteochondromas in the rib cage

To investigate the effect of HS deficiency on articular cartilage, we examined the skeletal phenotype of *Prg4-Cre*;*Ext1*$^{f/f}$ mice (hereafter called *Ext1*-cKO mice) and control littermates (hereafter called WT). In 3-month-old *Ext1*-cKO mice, skeletal deformities or multiple bony protrusions involving the upper and lower limbs were not identified through radiographic observations and analysis of whole-mount skeletal preparations [Fig. 2(A) and (B)]. However, *Ext1*-cKO mice presented with osteochondroma (arrowheads) development in the chondro-osseous junction in the rib cage [Fig. 2(C)]. We harvested knee joints, ribs and ankles and processed the resulting longitudinal serial sections for Safranin O/Fast Green staining. In *Ext1*-cKO mice, hypertrophic chondrocytes (arrowheads) were observed in the

articular cartilage [Fig. 2(D) and (E)] and costal cartilage [Fig. 2(G)]. However, abnormal morphologies were not detected in the growth plate cartilage tissues from *Ext1*-cKO mice [Fig. 2(F)].

Articular cartilage in Ext1-cKO mice expresses markers of hypertrophic chondrocytes

Immunohistochemistry was performed to accurately define the characteristics and phenotype of chondrocytes affected by HS loss-of-function. In *Ext1*-cKO mice, hypertrophic chondrocytes (arrowheads) expressed the hypertrophic marker Col10 and degenerative markers MMP-13 and ADAMTS-5 [Fig. 3(A)]. The chondrogenic marker Col2 was expressed around the hypertrophic chondrocytes [Fig. 3(A)].

Furthermore, we examined apoptosis in hypertrophic chondrocytes through TUNEL assays. TUNEL-positive hypertrophic chondrocytes were not detected in *Ext1*-cKO mice [Fig. 3(B)]. These results show that the hypertrophic phenotype did not induce apoptosis in chondrocytes.

HS chains regulate the activity of growth factor signaling in a cell-autonomous and/or non-cell-autonomous manner[37]. To evaluate the contribution of *Ext1*-null chondrocytes to hypertrophic chondrocytes, we performed fate-mapping analysis using *Prg4-Cre;Ext1*$^{f/f}$ mice harboring the *R26R* reporter gene. We monitored triple compound *Ext1*$^{f/f}$;*Prg4-Cre* in *R26R* mice (hereafter called cKO) and control littermate *Ext1*$^{f/f}$;*R26R* mice lacking the *Prg4-Cre* transgene (hereafter called control) and the knee joints of these mice were stained with X-gal to identify cells that had undergone Cre-mediated recombination. Hypertrophic chondrocytes contained variable numbers of lacZ + chondrocytes but never comprised 100% of lacZ + cells [Fig. 3(C)]. These results indicate that hypertrophic changes did not reflect the simple clonal growth of *Ext1*-null chondrocytes, suggesting that HS knock-out chondrocytes did not function in a cell-autonomous manner.

Hypertrophic chondrocytes and articular cartilage thickness are increased in Ext1-cKO mice at different ages

We assessed *Ext1*-cKO mice at different ages: P0, P14, P1M, P3M, P6M, and P12M. Samples from *Ext1*-cKO mice and age-matched littermate controls were subjected to staining with Safranin O/Fast Green to evaluate articular cartilage in the knee joint. Alterations in the cartilage structure of P0 mice were not detected. The first sign of abnormality was observed at P14, when hypertrophic chondrocytes emerged on the articular surface [Fig. 4(A)]. The %HC in the articular cartilage tissues significantly increased in *Ext1*-cKO mice compared to that in the controls at P1M, P3M, P6M, and P12M (*P*-value for the main effect (group) < 0.001, Fig. 4(B) and Supplementary Table S1). However, the interaction term between groups and ages was not significant ($P = 0.470$), as were not the differences in the %HC between ages (*P*-value for the main effect (age) = 0.393). These results indicated that there was no age-related significant difference in both *Ext1*-cKO and control groups.

The average articular cartilage thickness of *Ext1*-cKO mice in both the femoral condyle and the tibial plateau was significantly greater at P1M, P3M, P6M, and P12M (*P*-value for the main effect (group) = 0.007 and 0.002, respectively, Fig. 4(C) and Supplementary Table S2).

From P3M to P12M, the OARSI scores significantly increased in both WT (0.3 ± 0.5 to 1.9 ± 0.8; 95% CI 0.4 to 2.8, $P = 0.027$) and *Ext1*-cKO mice (0.8 ± 0.5 to 2.4 ± 0.5; 95% CI 0.5 to 2.7, $P = 0.023$), indicating spontaneous cartilage degeneration (*P*-value for the main effect (age) < 0.001). Of note, at every time point, the OARSI scores revealed no significant differences between genotypes (*P*-value for main effect (group):0.45, Fig. 4(D) and Supplementary Table S3). Inter-observer reliability between the two observers for the OARSI system displayed a similarly high intra-class correlation coefficient (ICC = 0.95). Our findings indicate that an *Ext1* deletion increased the number of hypertrophic chondrocytes in the articular cartilage, which became thicker at P14. However, *Ext1*-cKO mice did not develop early spontaneous age-related OA at the 1-year follow-up examination.

To further examine the effect of increased hypertrophic chondrocytes on experimental OA progression in the articular cartilage, we used a well-established mouse model of post-traumatic OA[27]. At 8 weeks after DMM surgery, traumatic OA progression did not significantly differ between *Ext1*-cKO and WT mice (Fig. 4(E) and (F) and Supplementary Table S4). These data indicate that the degradation of articular cartilage in the knee joints of mice with both age-associated OA and post-traumatic OA did not differ between WT and *Ext1*-cKO mice.

Upregulated BMP signaling in cartilage of Ext1-cKO mice

To investigate the role of BMP signaling in a mouse model with the joint surface cartilage-specific deletion of *Ext1*, we performed immunohistochemistry for BMP-responsive markers. The number of pSmad1/5/9-positive chondrocytes was higher in the articular cartilage of *Ext1*-cKO mice [Fig. 5(A)]. Furthermore, pSmad1/5/9 upregulation occurred in the costal cartilage of *Ext1*-cKO mice [Fig. 5(B)].

To confirm these results, we investigated the association between BMP-Smad1/5/9-signaling activity through Western blot analysis using primary chondrocytes. As expected, primary cultured chondrocytes isolated from P14 *Ext1*-cKO mice also exhibited the significant upregulation of pSmad1/5/9 protein levels compared to those from WT littermates ($n = 6$ per genotype, difference in mean −1.0,95%CI −1.7 to −0.3; $P = 0.016$; Fig. 5(C) and (D)). These results indicate that chondrocyte hypertrophy was associated with enhanced BMP-Smad signaling, which might be attributed to the loss of HS in articular cartilage tissue.

BMP signaling antagonist suppresses chondrocyte hypertrophy in the cartilage of Ext1-cKO mice

To determine whether the pharmacological inhibition of BMP signaling suppresses the hypertrophic phenotype of articular cartilage, *Ext1*-cKO mice were intraperitoneally administered LDN-193189. First, to investigate the effect of drug treatment on osteochondroma formation, we harvested the rib cages from LDN-193189- and vehicle-treated mice and analyzed the skeletal preparations. In vehicle-treated mutant mice at the 5-week time point, the ribs displayed multiple bony protrusions (arrowheads, Fig. 6(A)). LDN-193189 treatment drastically reduced osteochondroma development and growth in mutant mice [Fig. 6(A)]. Furthermore, to analyze the effects of drug treatment on articular cartilage, knee joints from LDN-193189 and vehicle-treated mutant mice were histologically

assessed. Interestingly, LDN-193189 treatment significantly reduced both the abundance of hypertrophic chondrocytes and the thickness of articular cartilage in *Ext1*-cKO mice (Fig. 6(B)–(D) and Supplementary Table S5). To confirm that these changes were induced by the inhibition of BMP signaling, we examined pSmad1/5/9 expression through immunohistochemistry. As expected, LDN-193189-treated mice exhibited pSmad1/5/9 downregulation in articular cartilage [Fig. 6(E)]. These data indicate that administration of the BMP inhibitor suppressed chondrocyte hypertrophy in cartilage tissue and that the loss of HS in articular cartilage led to chondrocyte hypertrophy because of increased BMP/Smad signaling.

Discussion

Previous studies have described different conditional *Cre*-mediated Ext1 deletions in MHE-model mice, including *Col2a1-CreERT;Ext1*$^{f/f}$[13,38], *Prx1-Cre;Ext1*$^{f/f}$[39], *Aggrecan-CreER;Ext1*$^{f/f}$[24], *Fsp1-Cre; Ext1*$^{f/f}$[40], and *Gdf5-Cre;Ext1*$^{f/f}$[41]. Here, we generated a mouse model with an articular cartilage-specific *Ext1* deletion using *Prg4-Cre* transgenic mice and performed histological analysis to determine the effects of HS deficiency on and the functions of HS in articular cartilage. Our results indicate that articular cartilage-specific HS-cKO mice display increased chondrocyte hypertrophy and cartilage thickness with upregulation of matrix-degrading enzymes, including MMP-13 and ADAMTS-5.

Chondrocyte hypertrophic changes have been reported in both human OA and experimental OA models in numerous studies[14–17]. These changes play crucial roles in OA pathogenesis through protease-mediated cartilage degradation. Moreover, hypertrophic chondrocytes degrade their surroundings, as seen in OA, which is important for disease pathogenesis and progression[20]. Sgariglia *et al.* reported that the lack of HS in cartilage in *Col2a1-CreERT;Ext1*$^{f/f}$ mice leads to chondrocyte hypertrophy in the articular cartilage, a severe disorganization of chondrocyte columnar organization, and a shortened hypertrophic zone[38]. Some discrepancies between their study and the present study might have depended on the differences in Cre mice because *Prg4-Cre* was expressed in joint cartilage, not in the growth plate, as with *Col2a1-CreERT*. However, hypertrophic chondrocytes were also observed in articular cartilage. Therefore, HS-dependent factors (including BMPs) could be present in the joints, thereby contributing to ectopic chondrocyte hypertrophy and the initiation of an osteoarthritic-like phenotype.

Chondrocyte hypertrophic changes represent a pathognomonic hallmark of OA. Therefore, we examined whether the mutant mice generated herein present with OA. We found that age-related spontaneous OA did not develop early in *Ext1*-cKO mice at 1-year follow-up. Furthermore, in the DMM model, the degradation of articular cartilage did not significantly differ between mice with different genotypes. However, the reasons as to why our mutant mice did not present with OA remain unclear. HS is a sulfated linear polysaccharide with a backbone of alternating N-acetylglucosamine and glucuronic acid residues, which is covalently bound to various core proteins to form HS proteoglycans. HS binds various morphogens and growth factors and modulates their activity. Therefore, HS might be involved in OA progression after hypertrophic changes, and the loss of HS could be a key to prevent OA. Schmale *et al.* reported that patients with MHE might develop early-onset OA[7].

However, our results suggest that HS deficiency does not directly cause osteoarthritic changes. Shu *et al.* reported that HS deficiency in perlecan exon 3-null mice exerts chondroprotective effects in a post-traumatic mouse model of OA induced through destabilization of the medial menisci[11]. Some studies have reported that *in vitro* chondrocyte cultures treated with heparanase to eliminate HS deposit more glycosaminoglycan than control cultures[42,43]. Therefore, the loss of HS might serve as a chondroprotective effector in these mouse models. The hypertrophic chondrocytes of transgenic mice used herein could be distinct from hypertrophic chondrocytes normally observed in OA cartilage, because normal OA hypertrophic chondrocytes were present at the joint surface[44]; however, hypertrophic chondrocytes were observed not only at the joint surface, but also at the deep layer of the articular cartilage.

HS proteoglycans are necessary for FGF, vascular endothelial growth factor, and TGFβ signaling and participate in the formation of morphogen gradients including those of Ihh or BMPs[25,39,45–47]. The critical loss of full-length HS chains disrupts ligand–receptor interactions and ligand-diffusion gradients in several signaling pathways (e.g., Ihh, BMPs, FGF, and Wnt), resulting in the development of osteochondroma[48–50]. Among them, we focused on BMP signaling, considering that several reports have suggested that aberrant BMP signaling plays a role in osteochondroma formation[22–24,51–53]. Furthermore, the loss of HS enhances BMP signaling rather than suppressing it[22–24,54]; however, these findings remain debatable. The present results indicate that the loss of HS enhances BMP signaling in the articular cartilage of cartilage-specific HS-cKO mice. Matsumoto Y *et al.*[39] reported that the responsiveness to exogenous BMPs is attenuated in micromass cultures using *Prx1-Cre;Ext1*$^{f/f}$ mutant limb buds. They carried out examinations during the chondrogenic phase. The phenotype of their mutant mice exhibited abnormal morphology and patterning at E13.5; however, these abnormalities were almost recovered at E16.5. Therefore, after the postnatal period, numerous studies, including the present study, indicate that the loss of HS enhances BMP signaling, and these discrepancies might result from the degree of tissue maturity.

The systemic administration of a BMP antagonist inhibits osteochondroma growth in MHE-model mice[23,24]. Inubushi *et al.*[23] reported that administration of the small-molecule BMP inhibitor LDN-193189 suppresses osteochondroma formation in mutant mice. Furthermore, Sinha *et al.*[24] reported that LDN-193189 treatment markedly reduces growth of the cartilaginous portion of osteochondromas, including cranial base osteochondroma. However, they did not report the effect of LDN-193189 on articular cartilage. In addition, our study is the first to show that the administration of a BMP inhibitor reduces the number of hypertrophic chondrocytes in the articular cartilage of cartilage-specific HS-cKO mice, along with the articular cartilage thickness. Thus, HS deficiency might lead to chondrocyte hypertrophy by increasing BMP signaling. HS plays an important role in maintaining the cartilaginous matrix by regulating BMP signaling.

This study has several limitations. This includes a risk of bias owing to a small sample size. Because hypertrophic chondrocytes in the articular cartilage of *Ext1*-cKO mice were markedly increased, OARSI scoring and the measurements of cartilage thickness and % HC were not blinded herein.

In summary, this study shows that HS deficiency in articular chondrocytes leads to chondrocyte hypertrophy in mice with a cartilage-specific *Ext1* deletion and that upregulated BMP/Smad signaling might partly contribute to this phenotype. Furthermore, this study shows that administration of the BMP inhibitor LDN-193189 significantly decreases the number of hypertrophic chondrocytes and cartilage thickness. These findings suggest that HS plays an important role in maintaining the cartilaginous matrix by regulating BMP signaling and could improve the understanding of the mechanisms underlying MHE. Our results will potentially guide further studies on novel pharmacotherapies for MHE.

Supplementary Material

Refer to Web version on PubMed Central for supplementary material.

Acknowledgments

Funding sources

This study was supported by a Grant-in-Aid for Scientific Research (JSPS KAKENHI grant number JP15K10446 to KM) and NIH grants R01AR055670 (to YY). The sponsors had no role in the study design, collection, analysis, and interpretation of data, writing of the manuscript, or the decision to submit the manuscript for publication.

References

1. Kim BT, Kitagawa H, Tanaka J, Tamura J, Sugahara K. *In vitro* heparan sulfate polymerization: crucial roles of core protein moieties of primer substrates in addition to the EXT1-EXT2 interaction. J Biol Chem 2003;278:41618–23. [PubMed: 12907685]
2. Jamsheer A, Socha M, Sowinska-Seidler A, Telega K, Trzeciak T, Latos-Bielenska A. Mutational screening of EXT1 and EXT2 genes in Polish patients with hereditary multiple exostoses. J Appl Genet 2014;55:183–8. [PubMed: 24532482]
3. Sarrion P, Sangorrin A, Urreizti R, Delgado A, Artuch R, Martorell L, et al. Mutations in the EXT1 and EXT2 genes in Spanish patients with multiple osteochondromas. Sci Rep 2013;3 1346. [PubMed: 23439489]
4. Ishimaru D, Gotoh M, Takayama S, Kosaki R, Matsumoto Y, Narimatsu H, et al. Large-scale mutational analysis in the EXT1 and EXT2 genes for Japanese patients with multiple osteochondromas. BMC Genet 2016;17 52. [PubMed: 26961984]
5. Xu L, Xia J, Jiang H, Zhou J, Li H, Wang D, et al. Mutation analysis of hereditary/multiple exostoses in the Chinese. Hum Genet 1999;105:45–50. [PubMed: 10480354]
6. Jennes I, Pedrini E, Zuntini M, Mordenti M, Balkassmi S, Asteggiano CG, et al. Multiple osteochondromas: mutation update and description of the multiple osteochondromas mutation database (MOdb). Hum Mutat 2009;30:1620–7. [PubMed: 19810120]
7. Schmale GA, Conrad EU 3rd, Raskind WH. The natural history of hereditary multiple exostoses. J Bone Jt Surg Am Vol 1994;76:986–92.
8. Matsumoto Y, Matsumoto K, Harimaya K, Okada S, Doi T, Iwamoto Y. Scoliosis in patients with multiple hereditary exostoses. Eur Spine J 2015;24:1568–73. [PubMed: 25794701]
9. Jones KB. Glycobiology and the growth plate: current concepts in multiple hereditary exostoses. J Pediatr Orthop 2011 ;31:577–86. [PubMed: 21654469]
10. Jones KB, Datar M, Ravichandran S, Jin H, Jurrus E, Whitaker R, et al. Toward an understanding of the short bone phenotype associated with multiple osteochondromas. J Orthop Res 2013;31:651–7. [PubMed: 23192691]
11. Shu CC, Jackson MT, Smith MM, Smith SM, Penm S, Lord MS, et al. Ablation of perlecan domain 1 heparan sulfate reduces progressive cartilage degradation, synovitis, and osteophyte size in a preclinical model of posttraumatic osteoarthritis. Arthritis & Rheumatology 2016;68:868–79. [PubMed: 26636652]

12. Inatani M, Irie F, Plump AS, Tessier-Lavigne M, Yamaguchi Y. Mammalian brain morphogenesis and midline axon guidance require heparan sulfate. Science 2003;302:1044–6. [PubMed: 14605369]
13. Matsumoto K, Irie F, Mackem S, Yamaguchi Y. A mouse model of chondrocyte-specific somatic mutation reveals a role for Ext1 loss of heterozygosity in multiple hereditary exostoses. Proc Natl Acad Sci U S A 2010;107:10932–7. [PubMed: 20534475]
14. van der Kraan PM, Blaney Davidson EN, Blom A, van den Berg WB. TGF-beta signaling in chondrocyte terminal differentiation and osteoarthritis: modulation and integration of signaling pathways through receptor-Smads. Osteoarthritis Cartilage 2009;17:1539–45. [PubMed: 19583961]
15. Tchetina EV, Kobayashi M, Yasuda T, Meijers T, Pidoux I, Poole AR. Chondrocyte hypertrophy can be induced by a cryptic sequence of type II collagen and is accompanied by the induction of MMP-13 and collagenase activity: implications for development and arthritis. Matrix Biol 2007;26: 247–58. [PubMed: 17306969]
16. van Donkelaar CC, Wilson W. Mechanics of chondrocyte hypertrophy. Biomech Model Mechanobiol 2012;11:655–64. [PubMed: 21847614]
17. Pesesse L, Sanchez C, Delcour JP, Bellahcene A, Baudouin C, Msika P, et al. Consequences of chondrocyte hypertrophy on osteoarthritic cartilage: potential effect on angiogenesis. Osteoarthritis Cartilage 2013;21:1913–23. [PubMed: 23973427]
18. von der Mark K, Kirsch T, Nerlich A, Kuss A, Weseloh G, Gluckert K, et al. Type X collagen synthesis in human osteoarthritic cartilage. Indication of chondrocyte hypertrophy. Arthritis & Rheumatology 1992;35:806–11.
19. Nurminskaya M, Linsenmayer TF. Identification and characterization of up-regulated genes during chondrocyte hypertrophy. Dev Dynam 1996;206:260–71.
20. van der Kraan PM, van den Berg WB. Chondrocyte hypertrophy and osteoarthritis: role in initiation and progression of cartilage degeneration? Osteoarthritis Cartilage 2012;20: 223–32. [PubMed: 22178514]
21. Zhong L, Huang X, Karperien M, Post JN. The regulatory role of signaling crosstalk in hypertrophy of MSCs and human articular chondrocytes. Int J Mol Sci 2015;16:19225–47. [PubMed: 26287176]
22. Huegel J, Sgariglia F, Enomoto-Iwamoto M, Koyama E, Dormans JP, Pacifici M. Heparan sulfate in skeletal development, growth, and pathology: the case of hereditary multiple exostoses. Dev Dynam 2013;242:1021–32.
23. Inubushi T, Nozawa S, Matsumoto K, Irie F, Yamaguchi Y. Aberrant perichondrial BMP signaling mediates multiple osteochondromagenesis in mice. JCI Insight 2017;2 e90049.
24. Sinha S, Mundy C, Bechtold T, Sgariglia F, Ibrahim MM, Billings PC, et al. Unsuspected osteochondroma-like outgrowths in the cranial base of hereditary multiple exostoses patients and modeling and treatment with a BMP antagonist in mice. PLoS Genet 2017;13 e1006742. [PubMed: 28445472]
25. Huegel J, Mundy C, Sgariglia F, Nygren P, Billings PC, Yamaguchi Y, et al. Perichondrium phenotype and border function are regulated by Ext1 and heparan sulfate in developing long bones: a mechanism likely deranged in hereditary multiple exostoses. Dev Biol 2013;377:100–12. [PubMed: 23458899]
26. Soriano P Generalized lacZ expression with the ROSA26 Cre reporter strain. Nat Genet 1999;21:70–1. [PubMed: 9916792]
27. Glasson SS, Blanchet TJ, Morris EA. The surgical destabilization of the medial meniscus (DMM) model of osteoarthritis in the 129/SvEv mouse. Osteoarthritis Cartilage 2007;15:1061–9. [PubMed: 17470400]
28. Yu PB, Deng DY, Lai CS, Hong CC, Cuny GD, Bouxsein ML, et al. BMP type I receptor inhibition reduces heterotopic ossification. Nat Med 2008;14:1363–9. [PubMed: 19029982]
29. Glasson SS, Chambers MG, Van Den Berg WB, Little CB. The OARSI histopathology initiative – recommendations for histological assessments of osteoarthritis in the mouse. Osteoarthritis Cartilage 2010;18:S17–23.

30. Jia H, Ma X, Tong W, Doyran B, Sun Z, Wang L, et al. EGFR signaling is critical for maintaining the superficial layer of articular cartilage and preventing osteoarthritis initiation. Proc Natl Acad Sci U S A 2016;113:14360–5. [PubMed: 27911782]
31. Xie L, Lin AS, Levenston ME, Guldberg RE. Quantitative assessment of articular cartilage morphology via EPIC-microCT. Osteoarthritis Cartilage 2009;17:313–20. [PubMed: 18789727]
32. Salvat C, Pigenet A, Humbert L, Berenbaum F, Thirion S. Immature murine articular chondrocytes in primary culture: a new tool for investigating cartilage. Osteoarthritis Cartilage 2005;13:243–9. [PubMed: 15727891]
33. Otsuki S, Hanson SR, Miyaki S, Grogan SP, Kinoshita M, Asahara H, et al. Extracellular sulfatases support cartilage homeostasis by regulating BMP and FGF signaling pathways. Proc Natl Acad Sci U S A 2010;107:10202–7. [PubMed: 20479257]
34. Ogawa H, Kozhemyakina E, Hung HH, Grodzinsky AJ, Lassar AB. Mechanical motion promotes expression of Prg4 in articular cartilage via multiple CREB-dependent, fluid flow shear stress-induced signaling pathways. Gene Dev 2014;28: 127–39. [PubMed: 24449269]
35. Rhee DK, Marcelino J, Baker M, Gong Y, Smits P, Lefebvre V, et al. The secreted glycoprotein lubricin protects cartilage surfaces and inhibits synovial cell overgrowth. J Clin Invest 2005;115:622–31. [PubMed: 15719068]
36. Kozhemyakina E, Zhang M, Ionescu A, Ayturk UM, Ono N, Kobayashi A, et al. Identification of a Prg4-expressing articular cartilage progenitor cell population in mice. Arthritis & Rheumatology 2015;67:1261–73. [PubMed: 25603997]
37. Hacker U, Nybakken K, Perrimon N. Heparan sulphate proteoglycans: the sweet side of development. Nat Rev Mol Cell Biol 2005;6:530–41. [PubMed: 16072037]
38. Sgariglia F, Candela ME, Huegel J, Jacenko O, Koyama E, Yamaguchi Y, et al. Epiphyseal abnormalities, trabecular bone loss and articular chondrocyte hypertrophy develop in the long bones of postnatal Ext1-deficient mice. Bone 2013;57: 220–31. [PubMed: 23958822]
39. Matsumoto Y, Matsumoto K, Irie F, Fukushi J, Stallcup WB, Yamaguchi Y. Conditional ablation of the heparan sulfate-synthesizing enzyme Ext1 leads to dysregulation of bone morphogenic protein signaling and severe skeletal defects. J Biol Chem 2010;285:19227–34. [PubMed: 20404326]
40. Inubushi T, Lemire I, Irie F, Yamaguchi Y. Palovarotene inhibits osteochondroma formation in a mouse model of multiple hereditary exostoses. J Bone Miner Res 2018;33:658–66. [PubMed: 29120519]
41. Mundy C, Yasuda T, Kinumatsu T, Yamaguchi Y, Iwamoto M, Enomoto-Iwamoto M, et al. Synovial joint formation requires local Ext1 expression and heparan sulfate production in developing mouse embryo limbs and spine. Dev Biol 2011;351:70–81. [PubMed: 21185280]
42. Huegel J, Enomoto-Iwamoto M, Sgariglia F, Koyama E, Pacifici M. Heparanase stimulates chondrogenesis and is up-regulated in human ectopic cartilage: a mechanism possibly involved in hereditary multiple exostoses. Am J Pathol 2015;185:1676–85. [PubMed: 25863260]
43. Nakamura R, Nakamura F, Fukunaga S. Disruption of endogenous perlecan function improves differentiation of rat articular chondrocytes in vitro. Anim Sci J 2015;86:449–58. [PubMed: 25410015]
44. Kamekura S, Hoshi K, Shimoaka T, Chung U, Chikuda H, Yamada T, et al. Osteoarthritis development in novel experimental mouse models induced by knee joint instability. Osteoarthritis Cartilage 2005;13:632–41. [PubMed: 15896985]
45. Stickens D, Zak BM, Rougier N, Esko JD, Werb Z. Mice deficient in Ext2 lack heparan sulfate and develop exostoses. Development 2005;132:5055–68. [PubMed: 16236767]
46. Koziel L, Kunath M, Kelly OG, Vortkamp A. Ext1-dependent heparan sulfate regulates the range of Ihh signaling during endochondral ossification. Dev Cell 2004;6:801–13. [PubMed: 15177029]
47. Nadanaka S, Kitagawa H. Heparan sulphate biosynthesis and disease. J Biochem 2008;144:7–14. [PubMed: 18367479]
48. Bornemann DJ, Park S, Phin S, Warrior R. A translational block to HSPG synthesis permits BMP signaling in the early Drosophila embryo. Development 2008;135:1039–47. [PubMed: 18256192]
49. Bornemann DJ, Duncan JE, Staatz W, Selleck S, Warrior R. Abrogation of heparan sulfate synthesis in Drosophila disrupts the wingless, hedgehog and decapentaplegic signaling pathways. Development 2004;131:1927–38. [PubMed: 15056609]

50. Bishop JR, Schuksz M, Esko JD. Heparan sulphate proteoglycans fine-tune mammalian physiology. Nature 2007;446:1030–7. [PubMed: 17460664]

51. Hecht JT, Hogue D, Strong LC, Hansen MF, Blanton SH, Wagner M. Hereditary multiple exostosis and chondrosarcoma: linkage to chromosome II and loss of heterozygosity for EXT-linked markers on chromosomes II and 8. Am J Hum Genet 1995;56:1125–31. [PubMed: 7726168]

52. Jochmann K, Bachvarova V, Vortkamp A. Heparan sulfate as a regulator of endochondral ossification and osteochondroma development. Matrix Biol 2014;34:55–63. [PubMed: 24370655]

53. Lin X Functions of heparan sulfate proteoglycans in cell signaling during development. Development 2004;131: 6009–21. [PubMed: 15563523]

54. Billings PC, Pacifici M. Interactions of signaling proteins, growth factors and other proteins with heparan sulfate: mechanisms and mysteries. Connect Tissue Res 2015;56:272–80. [PubMed: 26076122]

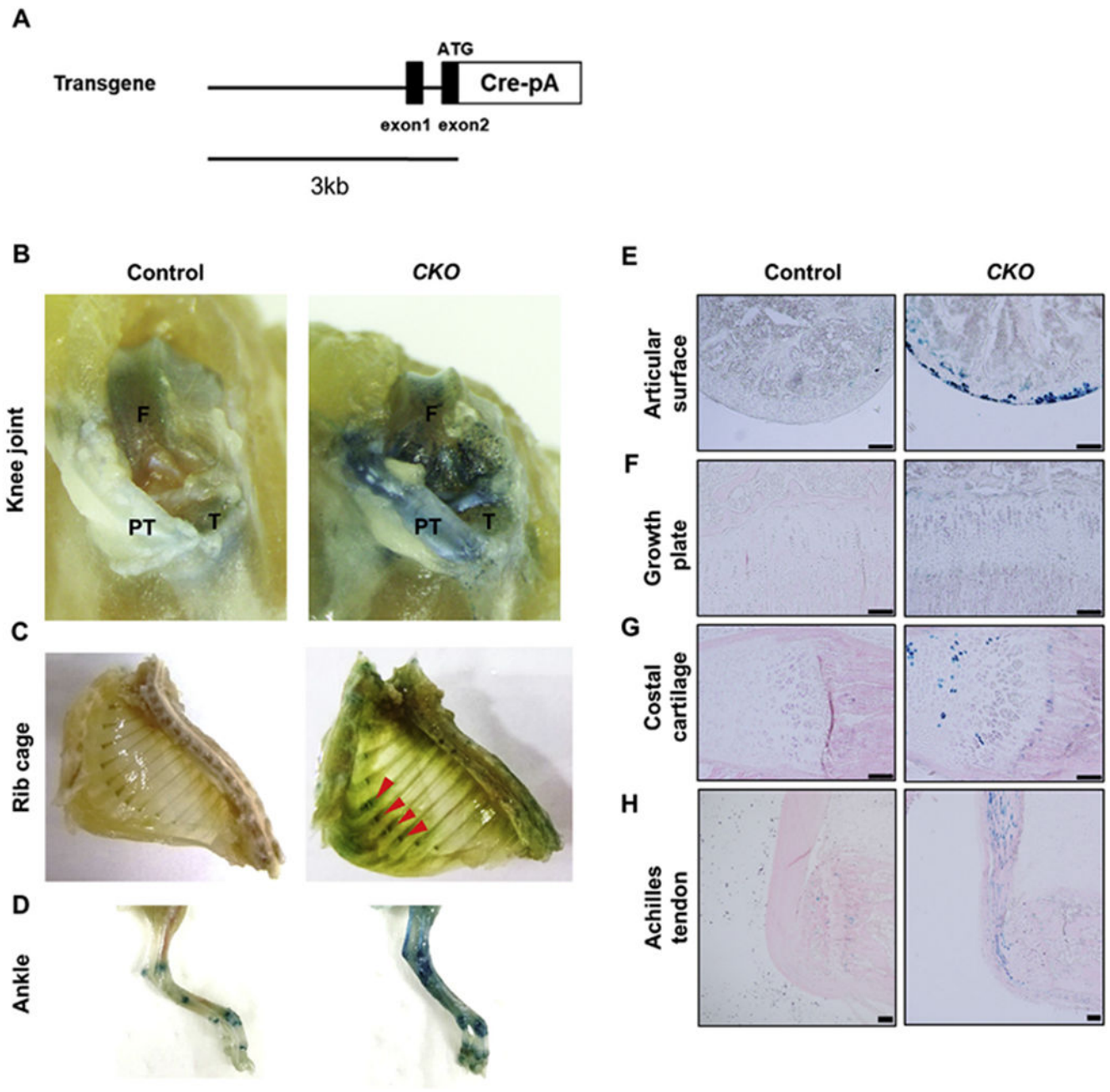

Fig. 1. ***Prg4-Cre*-mediated recombination in superficial articular chondrocytes.**

A, Schematic representation of construction of ***Prg4-Cre*** mice. **B**–**D**, ***Prg4-Cre;Rosa26***-lacZ mice (cKO) and their control littermates (control) were euthanized on postnatal day 28 (P28), followed by whole-mount X-Gal staining. X-Gal-stained whole mounts of knee joints (F, femur; T, tibia; P, patellar tendon) (**B**), rib cages (**C**), and ankles (**D**) obtained on P28. **E**–**H**, Sections of the femoral articular cartilage (**E**), tibial growth plates (**F**), costal cartilage (**G**), and Achilles tendons (**H**) from control and ***Prg4-Cre;Rosa26***-lacZ mice are shown. Scale bars = 100 μm (**E**–**H**).

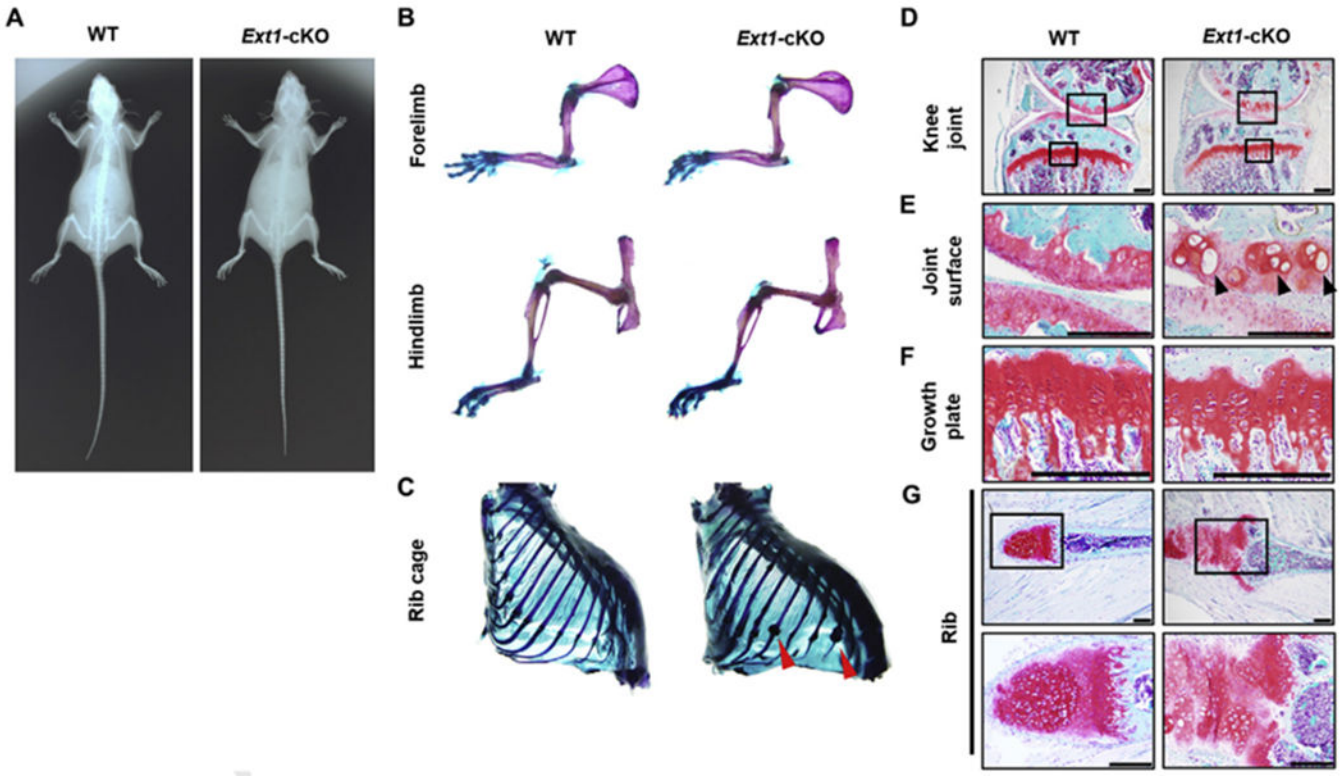

Fig. 2. Cartilage-specific *Ext1*-conditional-knockout mice display hypertrophic chondrocytes of articular cartilage.

A, X-ray images of 3-month-old ***Ext1***-cKO mice and their control littermates (WT). **B** and **C**, Whole-mount skeletal preparations of limbs (B) and rib cages (**C**) from ***Ext1***-cKO and WT mice. ***Ext1***-cKO mice did not display bony protrusions in the forelimbs and hindlimbs but did show osteochondromas in the chondro-osseous junction of the rib cage. **D**–**G**, Safranin O/Fast Green-stained sections of the knee joints (**D**), joint surfaces (**E**), growth plates (**F**) and rib bones (**G**) of 3-month-old ***Ext1***-cKO and WT mice. The number of hypertrophic chondrocytes increased in the articular cartilage and costal cartilage. Abnormal morphology of the growth plate was not observed. Scale bars = 200 μm. The data shown are representative images; each analysis was performed on at least four animals per genotype.

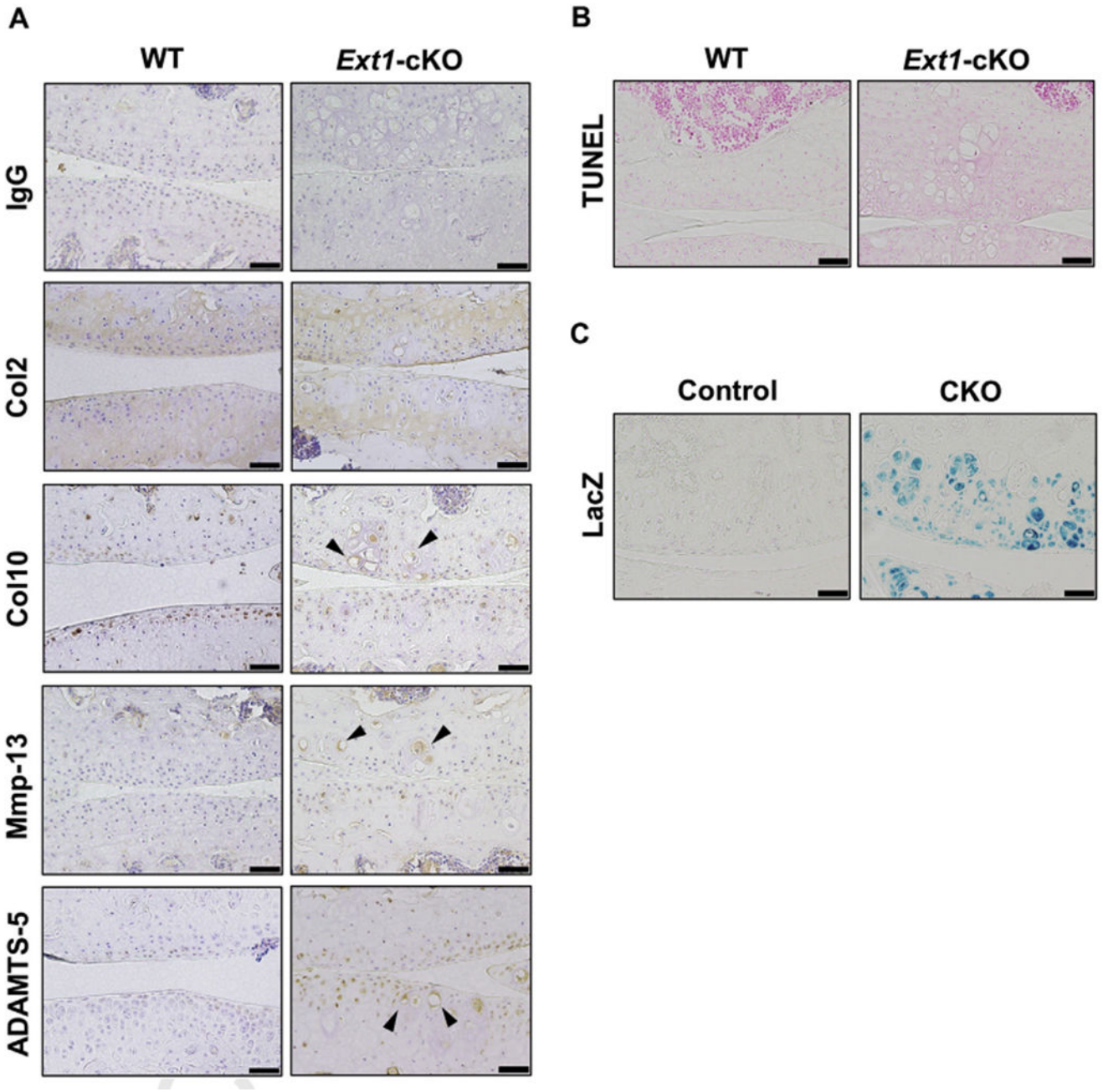

Fig. 3. Hypertrophic chondrocytes in cartilage-specific *Ext1*-cKO mice display expression of hypertrophic (Col10) and degenerative (MMP-13 and ADAMTS-5) markers.

A, Immunostaining for Col2, Col10, MMP-13, and ADAMTS-5 in cartilage sections from 3-month-old ***Ext1***-cKO mice and their control littermates (WT). Normal rabbit IgG was used as a negative control. In ***Ext1***-cKO mice, hypertrophic chondrocytes displayed expression of a hypertrophic marker (Col10) and two degenerative markers (MMP-13 and ADAMTS-5). **B**, Evaluation of hypertrophic chondrocyte apoptosis. Terminal deoxynucleotidyl transferase dUTP nick end labeling (TUNEL) staining of articular cartilages from 3-month-old ***Ext1***-cKO and WT mice. TUNEL-positive hypertrophic chondrocytes were not detected in ***Ext1***-

cKO mice. **C**, Fate-mapping analysis of hypertrophic chondrocytes using ***R26R;Prg4-Cre;Ext1f/f*** compound mice was performed. X-gal staining of articular cartilages from ***R26R;Prg4-Cre;Ext1f/f*** compound mice (cKO) and their control littermates (control). ***Prg4***-expressing cells did not necessarily change in a hypertrophic manner. Scale bars = 50 μm (A–C). The data shown are representative images; each analysis was performed on at least four animals per genotype.

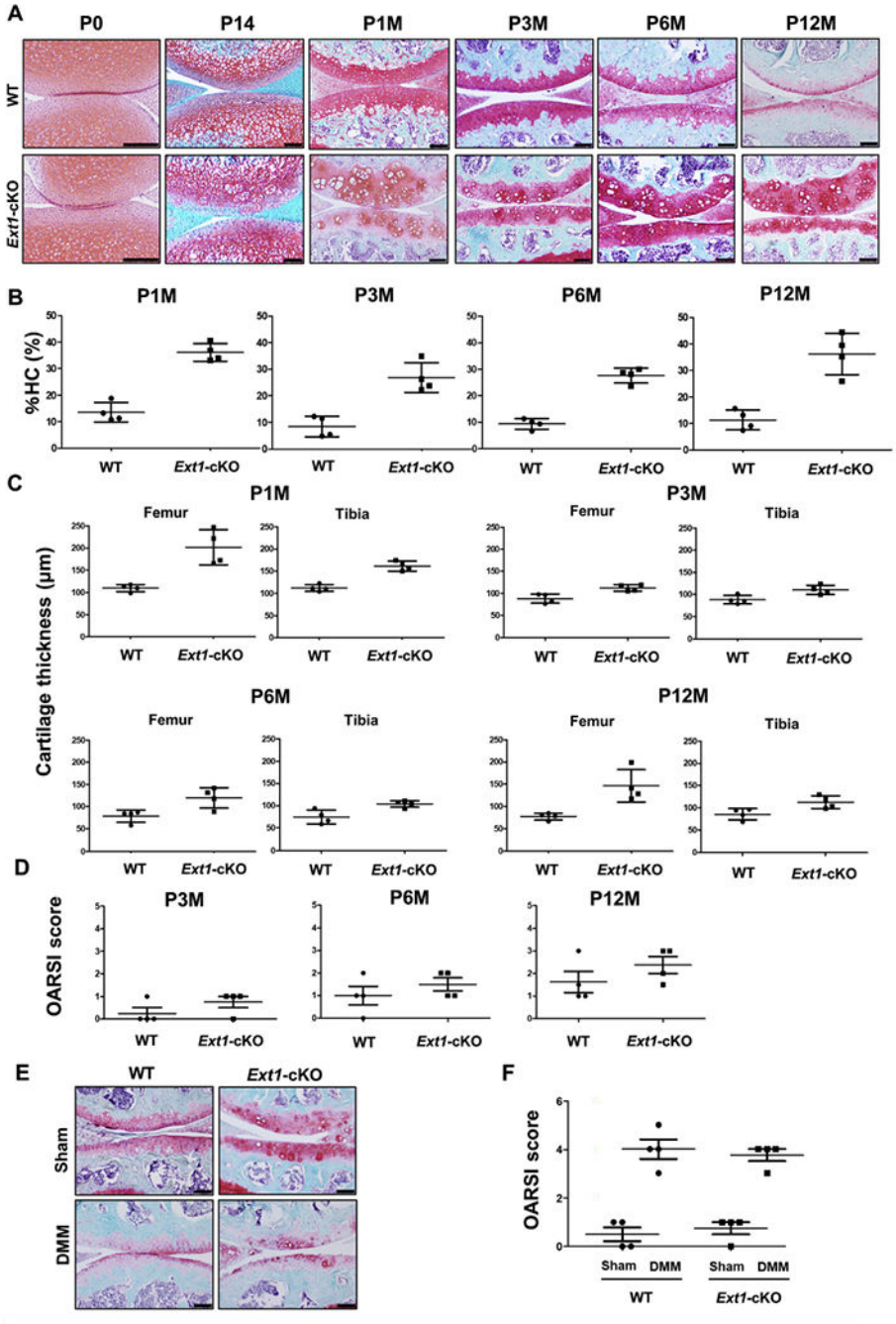

Fig. 4. Hypertrophic chondrocytes and the articular cartilage thickness increase in *Ext1*-conditional-knockout (cKO) mice at various ages.

A, Safranin O/Fast Green-stained knee joint sections of ***Ext1***-cKO mice and their control littermates (WT) at postnatal day 0 (P0), P14, postnatal month 1 (P1M), P3M, P6M, and P12M. Hypertrophic chondrocytes were observed in articular cartilage beginning at P14 in ***Ext1***-cKO mice. **B**, Percentage of hypertrophic chondrocytes (%HC) in both the femoral condyle and tibial plateau from P1M, P3M, P6M, and P12M ***Ext1***-cKO and WT mice (n = 4 per genotype at every time point). The % HC values in articular cartilage increased

significantly in ***Ext1***-cKO mice. **C**, Average thicknesses of articular cartilage in both the femoral condyle and tibial plateau from P1M, P3M, P6M, and P12M ***Ext1***-cKO and WT mice (n = 4 per genotype at every time point). Average thickness of the articular cartilage in both the femoral condyle and tibial plateau increased significantly in ***Ext1***-cKO mice. **D**, Osteoarthritis Research Society International (OARSI) scores in P3M, P6M, and P12M ***Ext1***-cKO and WT mice (n = 4 per genotype at every time point). OARSI scores did not significantly differ between genotypes at the 1-year follow-up timepoint. **E**, Safranin O/Fast Green staining of cartilage sections from ***Ext1***-cKO mice and their WT littermates 8 weeks after sham operation or surgical destabilization of the medial meniscus (DMM) are shown. **F**, OARSI grades in sham or DMM-operated WT (n = 4) and ***Ext1***-cKO mice (n = 4). OARSI scores did not significantly differ between genotypes. Scale bars = 100 μm (**A, F**).

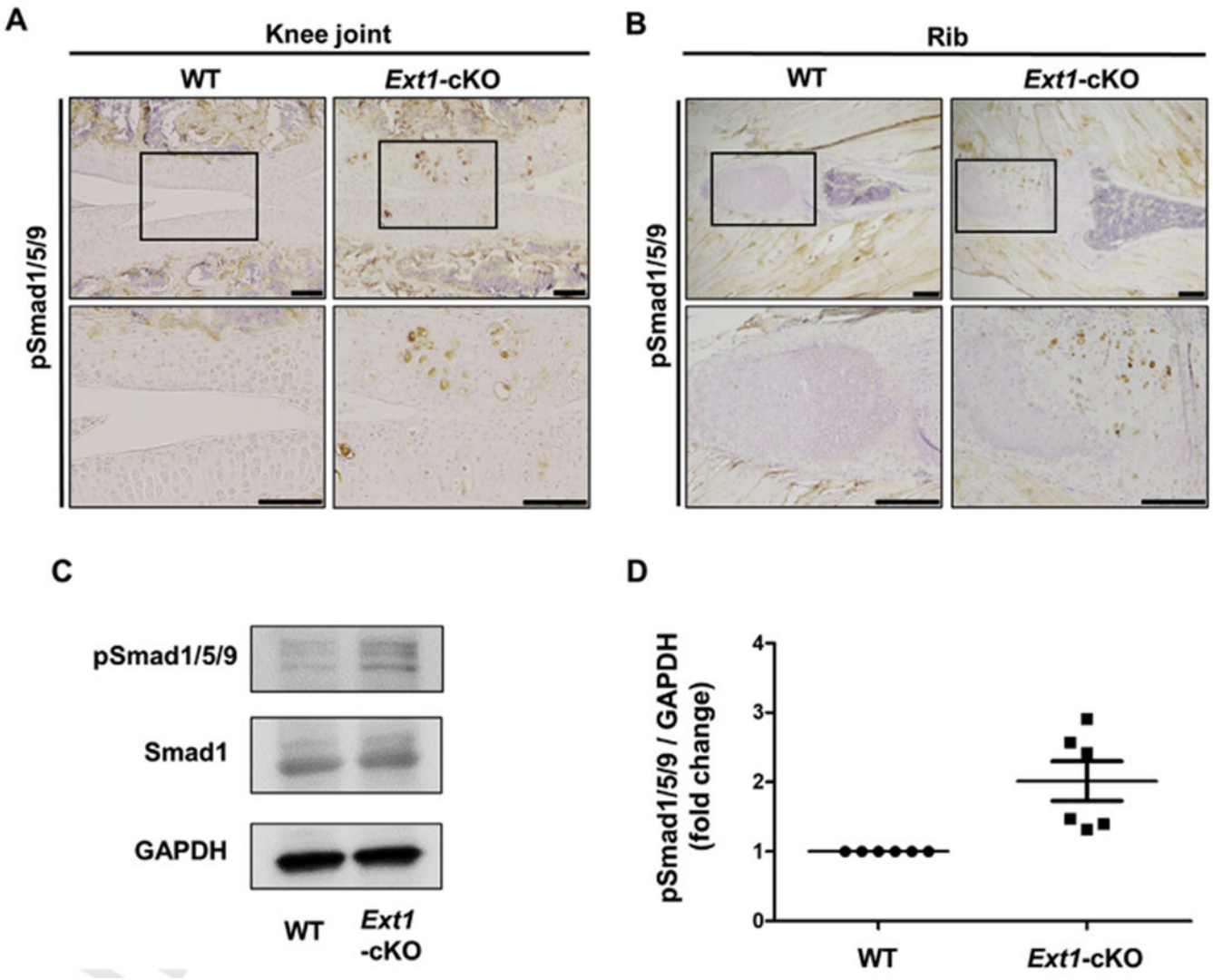

Fig. 5. Bone morphogenetic protein (BMP) signaling is upregulated in chondrocytes of cartilage-specific *Ext1*-conditional-knockout (cKO) mice.

A and **B**, pSmad1/5/9 expression in articular cartilage and costal cartilage. Sections of knee joints (**A**) and rib bones (**B**) from P1M ***Ext1-c***KO mice and their control littermates (WT) were stained with an anti-pSmad1/5/9 antibody. Upregulation of pSmad1/5/9 was observed both in articular and costal cartilage of ***Ext1***-cKO mice. **C**, Immunoblotting against pSmad1/5/9, Smad1, and GAPDH in protein extracts from primary chondrocytes from WT and ***Ext1***-cKO mice. **D**, Signal intensity of pSmad1/5/9 relative to that of GAPDH was quantified using NIH ImageJ software. Primary cultured chondrocytes isolated from ***Ext1***-cKO mice exhibited upregulation of pSmad1/5/9 protein levels compared to those from control littermates. Scale bars = 100 μm (**A** and **B**). Immunoblot analysis was performed for at least six mice per genotype, and representative images are shown.

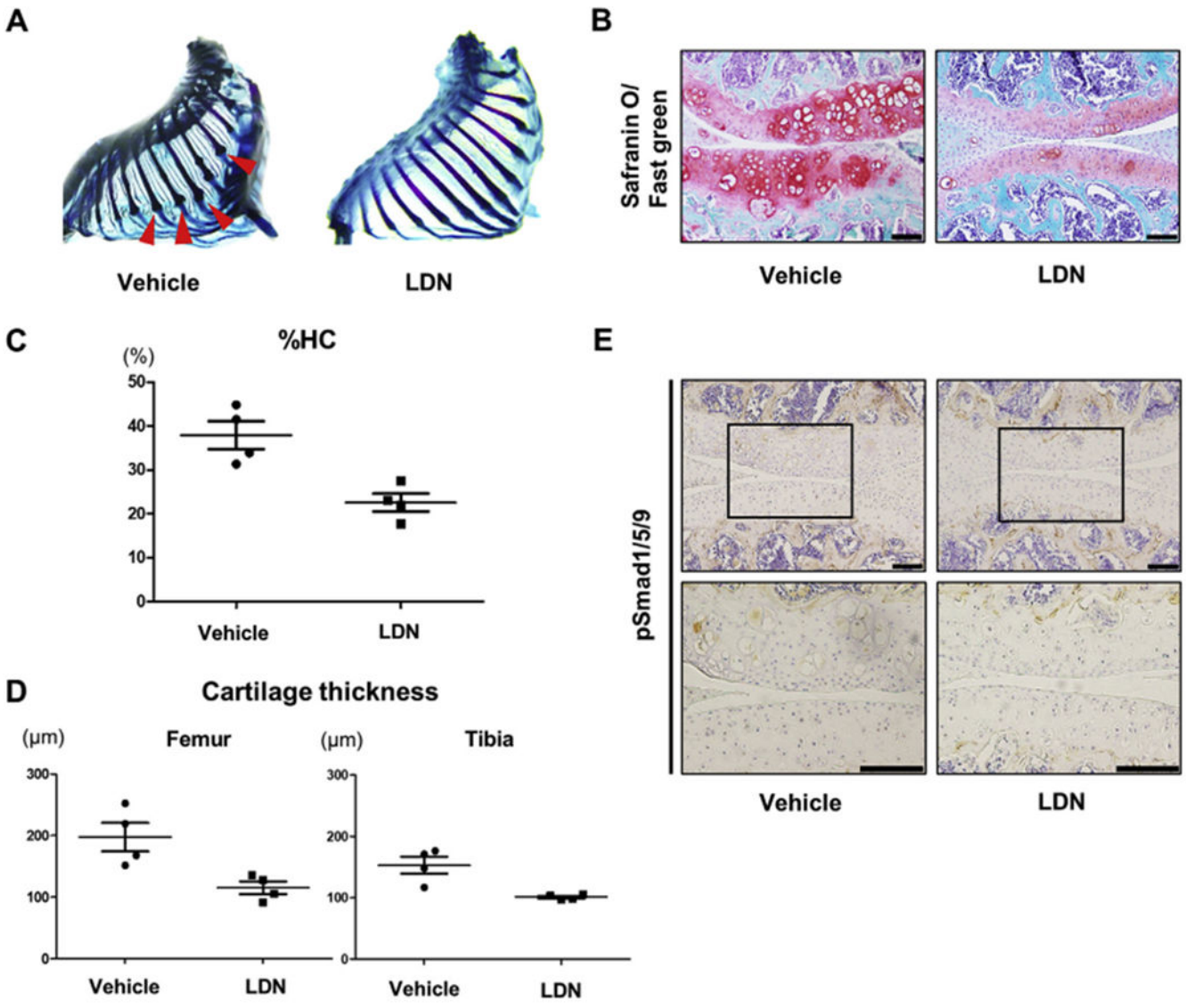

Fig. 6. Pharmacological inhibition of bone morphogenetic protein (BMP) with LDN-193189 suppresses chondrocyte hypertrophy in cartilage-specific *Ext1*-conditional knockout (cKO) mice.

A, Whole-mount skeletal preparations of the rib cage of LDN-193189-treated mutant mice and vehicle-treated mutant littermates at the end of drug treatment. LDN-193189 treatment effectively reduced osteochondroma development and growth in mutant mice. **B**, Safranin O-stained sections of the knee joint of LDN-193189- and vehicle-treated mice. Representative images were obtained from at least four mice per group. **C**, Percentage of hypertrophic chondrocyte (%HC) values for both the femoral condyle and tibial plateau from LDN-193189- and vehicle-treated mice were quantified (***n*** = 4 per group). LDN-193189-treated mutant mice showed a significantly reduced abundance of hypertrophic chondrocytes. **D**, Average thicknesses of articular cartilage in both the femoral condyle and tibial plateau from LDN-193189- and vehicle-treated mice were quantified (***n*** = 4 each group). LDN-193189 treatment significantly reduced the articular cartilage thicknesses **E**, pSmad1/5/9 expression in the articular cartilage of LDN-193189- and

vehicle-treated mutant mice. LDN-193189-treated mice exhibited pSmad1/5/9 downregulation in articular cartilage tissues. Representative images are shown. Scale bars = 100 μm (**B** and **E**).